Strength of Continuous Composite Beams Designed to Eurocode 4

Résistance des poutres mixtes acier-béton continues, calculée selon l'Eurocode 4

Tragfähigkeit von durchlaufenden Stahl-Beton-Verbundträgern, berechnet nach Eurocode 4

Roger Paul JOHNSON
Prof. of Civil Engineering
University of Warwick
Coventry, UK

R.P. Johnson was educated at Cambridge University. After six years in industry he began research on composite structures in 1959. He is a member of IABSE Working Commission 2, and of the Editorial Group for Eurocode 4 on Composite Structures.

C.K. Roger FAN
Research Student
University of Warwick
Coventry, UK

C.K.R. Fan graduated from City University (London) in 1982. After gaining three years' experience in the construction industry, he went to Imperial College, London, for postgraduate study and was awarded an M.Sc. in structural steel design in 1986.

SUMMARY

The 1985 draft of Eurocode 4 gave a new method for the design of continuous composite beams with semi-compact (Class 3) sections at internal supports, that allows limited redistribution of moments. The validity of this method is examined for ultimate and serviceability limit states, by means of a parametric study based on test data on the post-local-buckling behaviour of cantilevers. It is concluded that the method is safe and economical for beams of uniform section, used in buildings.

RÉSUMÉ

Le projet 1985 de l'Eurocode 4 présente une nouvelle méthode pour le calcul des poutres mixtes continues à section semi-compacte (classe 3), autorisant une redistribution limitée des moments sur appuis intermédiaires. La validité de la méthode est examinée aux états limites de service et de ruine, au moyen d'une étude paramétrique basée sur des résultats d'essais relatifs au comportement postcritique de poutres-console. Il est montré que la méthode est sûre et économique pour des poutres de section constante utilisées dans le bâtiment.

ZUSAMMENFASSUNG

Der Entwurf 1985 des Eurocodes 4 schlägt eine neue Methode für die Berechnung durchlaufender Verbundträger mit halb-kompaktem Querschnitt (Klasse 3) über den Zwischenauflager vor, welche eine begrenzte Momentenumlagerung zulässt. Der Gültigkeitsbereich dieser Methode wird für die Grenzzustände der Tragsicherheit und der Gebrauchstauglichkeit geprüft, und zwar durch eine Parameterstudie basierend auf Versuchsresultaten von Kragarmträgern mit überkritischem Beulverhalten. Es wird gezeigt, dass die Methode für Träger des Hochbaus mit konstantem Querschnitt sicher und wirtschaftlich sind.

1. INTRODUCTION

For the longer spans of continuous composite beams in buildings, it is common to use rolled or built-up steel I- or H-sections that are semi-compact at internal supports. These are sections that can reach the yield moment in hogging bending, M'_y, but lose strength due to local buckling before much plasticity or local rotation can develop.

In design to draft Eurocode 4 [1] these beams are in Class 3 and have web and compression flange slendernesses that lie within the limits shown in Figure 5. Design methods for Class 3 steel beams at the ultimate limit state require elastic analysis of the structure and of the Class 3 cross sections. This is over-restrictive for composite beams, which are usually in Class 1 or 2 at midspan, because M'_y is much less than the plastic resistance at midspan, M_p, whereas elastic global analysis gives support moments that exceed the midspan moments.

The less conservative of the two design methods for Class 3 beams given in clause 4.4.3.2 of the draft EC4 (Appendix D) therefore allows up to 20 per cent redistribution of hogging moments determined by elastic analysis, in the belief that local buckling, if it occurs, can be relied on to shed at least this amount of bending moment before collapse occurs. The midspan regions are required to remain elastic (which is rarely a constraint in practice), because any inelastic curvature would increase the demand on the limited rotation capacity available near the internal supports.

The objective of the work reported here was to check on the safety of this method, using the limited test data on the post-local-buckling behaviour of cantilevers with sections in Class 3. It was assumed that complete shear connection was provided, and that lateral buckling did not occur. The 43 beams studied were each of uniform section, and ten cross-sections were used. The results are believed to be applicable to beams that have composite floor slabs and/or lightweight-aggregate concrete, as well as to conventional T- and L-beams.

The disparity between the design moments given by elastic global analysis and design resistances of sections is normally greater in a two-span beam than in those continuous over three or more spans. The various patterns of imposed loading lead to the provision of more surplus strength in multi-span beams, and they have a higher degree of redundancy. Two-span beams benefit most from the exploitation of inelastic behaviour, so only they have been studied. The spans ranged from 6m to 20m, and the ratios of the two span lengths from 0.6 to 1.0. Loading was taken as uniformly-distributed over each span, but allowance was made for different intensities on the two spans.

There has been much research related to the design of continuous composite beams of compact section (Class 1 or 2), and a little on slender (Class 4) cross-sections [2]. Very little work has been done on Class 3 beams [3,4,5], probably because the complex interaction of flange and web local buckling affects the rotation capacity in hogging bending, and this effect is difficult to assess analytically. Climenhaga and Johnson [5] found from double-cantilever tests that specimens with Class 3 cross sections have a distinct type of behaviour. Rotation due to local buckling occurs only near the support, and the buckling extends over a length roughly equal to the depth of the steel section. Due to this localised feature, the moment-rotation behaviour of hogging moment regions of a continuous beam can be predicted from the results of double-cantilever tests.

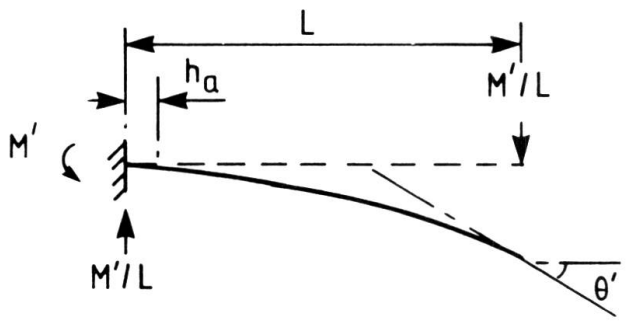

Fig. 1 M' – θ' relationship for a cantilever

2. OUTLINE OF THE METHOD OF ANALYSIS

(1) From tests on composite or steel cantilevers with point loads M'/L (Figure 1), curves are available (e.g., Figure 2) that relate the end slope θ' to the hogging bending moment at the support, M'.

It is assumed that θ' is the sum of an elastic rotation ($M'\theta'_e$/ M'_y in Figure

2), that can be found by integrating curvatures along the member, and an irreversible rotation θ'_i that occurs only in a region of length h_a adjacent to the support, where h_a is the overall depth of the steel member. The rotation θ'_i, due mainly to local buckling of the steel compression flange and/or web, is assumed to be the function of M'/M'_y and θ'_{bc} shown in Figure 2, and to occur at distance $h_a/2$ from the support.

(2) For a uniform composite or steel cantilever of any given length and cross section, the curve NP and values of M'_y, θ'_e, and θ'_{bc} are predicted, using realistic stress–strain curves for the materials and allowing for residual stresses in the steel section. The shape assumed for the falling branch, PQR in Figure 2, gives a close but conservative fit to the falling branches observed in the five tests studied. Details of these procedures are given in Appendix A.

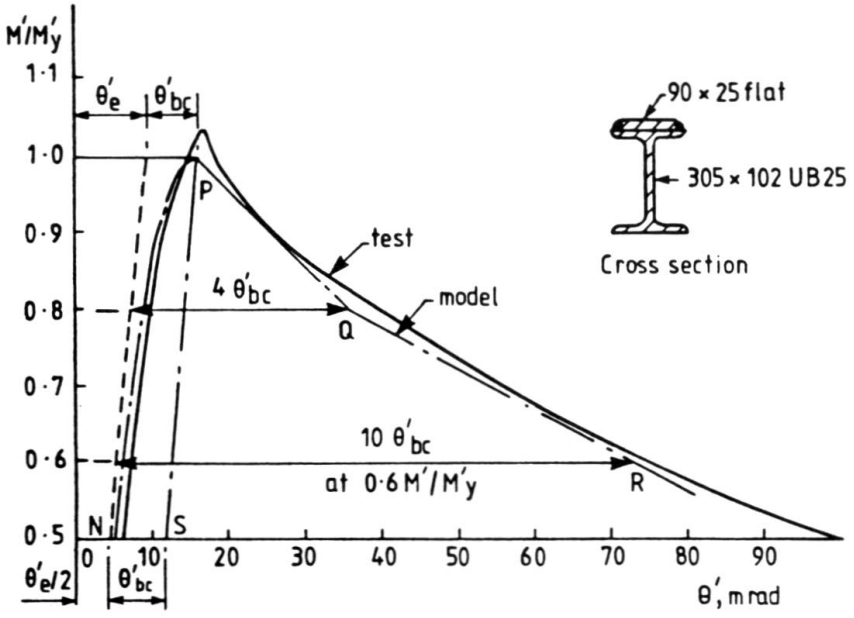

Fig. 2 Moment–rotation model compared with result of test on specimen SB4 [5] for a cantilever

(3) At an internal support of a continuous beam, the member is either stiffened, or interrupted by a column. There will be less redistribution of moments to midspan regions when local buckling occurs on one side only of the support, rather than on both sides. After M'_y has been reached at an internal support, the irreversible rotation is therefore assumed to remain constant (line PS in Figure 2) on the side with the steeper moment gradient, and to follow lines PQR on the other side.

Unlike a cantilever, a two–span continuous beam on point supports can rotate at the internal support, and the length of the hogging moment region reduces as redistribution of moments occurs. The rotation θ'_{bc} then has to be calculated in a different way, explained below and in Appendix C; so for continuous beams the symbol θ'_{bc} is replaced by θ'_b.

First, realistic spans L_1 and L_2 (with $L_2 \geq L_1$) and appropriate cross sections are chosen. The 'uncracked unreinforced' section for the beam is uniform over the whole length. The 'cracked reinforced' section is uniform over the hogging moment region, where the steel section is in Class 3 (semi–compact) as defined in draft Eurocode 4. All midspan sections are in Class 1 or Class 2.

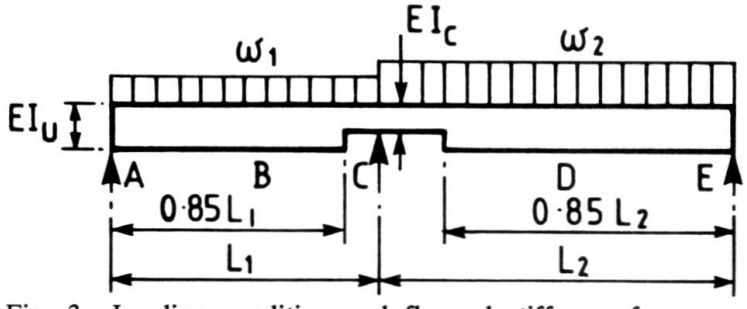

Fig. 3 Loading condition and flexural stiffness of a two–span beam

(4) The design ultimate loads, w_1 and w_2, are uniformly distributed, as shown in Figure 3. They are the maximum loads per unit length for which the beam could have been designed in accordance with the method of Appendix D.

The calculation of w_1 and w_2 is explained in Appendix B.

For span 1, the distributed characteristic dead and imposed loads per unit length are g_1 and q_1. It is assumed that w_1 can have any value between $1.0g_1$ and $1.35g_1 + 1.5q_1$, as the factors γ_F in the Eurocodes are expected to give a similar or lower range of loads. The range for span 2 is similar; g_2 is taken as equal to g_1, but q_2 may differ from q_1.

The designs are usually governed by the bending moments at first yield at cross-sections C (because a Class 3 section) and D (because the method excludes inelastic behaviour in midspan regions).

(5) The beam is now assumed to be subjected to loads λw_1 and λw_2, where λ increases gradually. Using analytical models based on research, and without reference to Eurocode 4, two values of λ are calculated (Appendix C):

(i) λ_b, at which the bending moment at support C reaches M'_y, and at which local buckling is assumed to occur; and

(ii) λ_f, at which "failure" (defined in Appendix C) occurs.

(6) The design method is assumed to be satisfactory, for the beam considered, if

(i) λ_b is high enough for local buckling not to occur at serviceability load levels, and

(ii) λ_f exceeds 1.0.

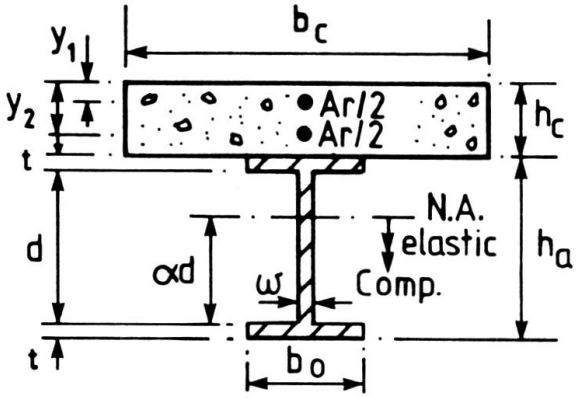

Fig. 4 Typical cross-section

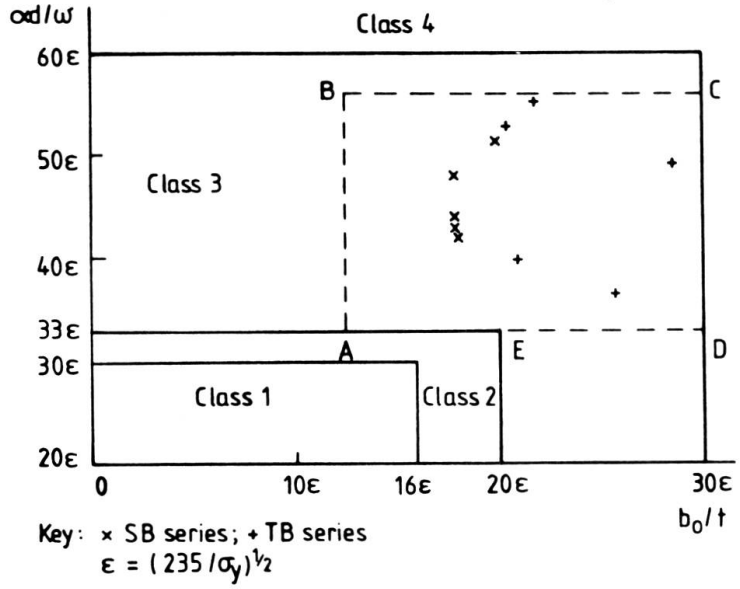

Fig. 5 Limiting slendernesses for cross-sections to Eurocode 4

3. CHOICE OF MEMBERS FOR STUDY

3.1 Cross sections

The notation for properties of cross sections is shown in Figure 4. For all sections, y_1 = 30mm and $y_2 = h_c - 30$mm. Rolled sections are replaced by three equivalent rectangles. The depth of web in compression, αd, was calculated (following draft Eurocode 4) using the elastic neutral axis. This method is under review; so is the specified maximum web slenderness for a Class 2 section ($\alpha d/w \leqslant 33\,\epsilon$, where $\epsilon = (235/\sigma_y)^{\frac{1}{2}}$, σ_y in N/mm² units) used here. The upper limit for a Class 3 web depends on the shear stress, but is unlikely to exceed 60ϵ. The current limits for webs and for compression flanges of rolled sections are shown in Figure 5. The practical range of Class 3 sections is given by the smaller area ABCDE.

The sections studied here (Tables 1 and 2) are five of the SB series tested by Climenhaga [5] and five (TB series) chosen to include the most slender hot-rolled beam sections that typically have Class 3 webs.

Section	b_o	t	w	d	b_o/t	$\alpha d/w$	σ_y	b_c	h_c	A_r	$10^{-6}I_c$	$10^{-6}I_u$
	mm	mm	mm	mm			N/mm²	mm	mm	mm²	mm⁴	mm⁴
SB4	103.5	7.34	6.0	298.5	14.1	34.5	386	1000	120	1200	91	196
SB5	127.5	8.56	6.0	334.3	14.9	39.8	343	1500	120	1836	155	309
SB6	141.2	8.43	6.2	385.8	16.7	42.7	340	1500	120	1818	214	423
SB10	103.5	7.34	6.0	298.5	14.1	33.0	386	1000	120	960	85	196
SB11	127.5	8.56	6.0	334.1	14.9	35.1	343	1500	120	954	127	308

Table 1 Properties of cross-sections SB

Section	b_o	t	w	d	b_o/t	$\alpha d/w$	σ_y	b_c	h_c	A_r	$10^{-6}I_c$	$10^{-6}I_u$
	mm	mm	mm	mm			N/mm²	mm	mm	mm²	mm⁴	mm⁴
TB1	171.0	9.7	6.9	332.6	17.6	44.9	355	2500	150	7500	336	516
TB2	141.8	8.6	6.3	380.1	16.5	43.2	355	2500	120	2250	226	454
TB3	146.1	8.6	6.1	234.3	17.0	32.4	355	2500	120	3000	105	206
TB4	350.0	15.0	10.0	650.0	23.3	40.0	355	2500	150	3750	1927	3669
TB5	315.0	15.0	10.0	500.0	21.0	29.6	355	2500	120	2400	950	1900

Table 2 Properties of cross-sections TB

3.2 Spans

Most continuous two-span Class 3 beams for buildings and footbridges have ratios of longer span to overall depth between 20 and 30, and spans between 6m and 20m. These ranges are explored in the 43 beams analysed, in which the ratios L_1/L_2 of shorter to longer span range from 0.6 to 1.0.

3.3 Materials

For the SB series, the yield stresses of the structural steel (Table 1) are based on the measured values for the relevant cantilever [5]. For the TB series, σ_y = 355 N/mm². For both series, f_y for reinforcement is 425 N/mm² and f_{cu} for the normal-density concrete is 30 N/mm². Details of the stress-strain curves and assumed residual stresses are given in Figures A1 and A2 (Appendix A).

Beam	L_1	L_2	Comp. M'_y	Obs. M'_m	Comp. θ'_b	Obs. θ'_{bc}	Comp. V/V_{pl}	Obs. V/V_{pl}
	m	m	kNm	kNm	mrad	mrad		
SB42	10.0	12.5	163.9	166.9	8.5	7.0	0.22	0.21
SB52	10.0	12.5	215.0	218.1	6.7	7.0	0.29	0.28
SB62	10.0	12.5	260.0	291.5	5.9	6.0	0.29	0.31
SB101	10.0	10.0	158.8	174.0	7.8	8.0	0.28	0.33
SB111	10.0	10.0	198.1	212.1	6.4	8.0	0.35	0.40

Table 3 Comparison between observed and computed results

Beam	L_1	L_2	Dead Load	w_1	w_2	λ_b	λ_f
	m	m	kN/m	kN/m	kN/m		
SB51	10.0	10.0	4.57	17.47	26.85	0.84	1.255
TB13	10.0	10.0	9.28	21.01	40.46	0.98	1.334
TB41	15.0	15.0	10.16	74.03	94.46	0.79	1.136
TB51	12.5	12.5	8.19	73.03	91.28	0.80	1.123

Table 4 Results for unpropped construction

4. RESULTS OF PARAMETRIC STUDY

4.1 Comparisons between cantilevers and two-span beams

Computed results M'_y, θ'_b, and maximum vertical shear V for five of the SB series of two-span beams are compared in Table 3 with the observed results from the tests on double cantilevers with the same cross sections and properties of materials. Propped construction was assumed.

The ratios V/V_{pl}, where $V_{pl} = \sigma_y dw/\sqrt{3}$, show that the effects of shear on flexural behaviour were negligible. The close agreement between θ'_b and θ'_{bc} shows that differences between their

methods of computation had negligible effect. At $V/V_{pl} = 0.2$ the computed value is slightly higher; at $V/V_{pl} = 0.3$ it agrees closely; at $V/V_{pl} = 0.4$ it is lower than the observed value, and so gives a more conservative model of the falling branch of the $M'-\theta'$ curve as V/V_{pl} increases. The observed maximum moments exceeded M'_y by between 1 and 12 per cent, so providing for most beams a further margin of safety.

4.2 Effect of unpropped construction

The four beams with two equal spans that gave the lowest values of λ_f (1.14, 1.07, 1.10, and 1.09) were also analysed using unpropped construction, with the results given in Table 4.

5. ANALYSIS AND DISCUSSION OF RESULTS FOR BEAMS

5.1 Load factors λ_b and λ_f

The load factor λ_b at the onset of local buckling was between 0.77 and 0.79 for all 43 beams with propped construction. This shows that local buckling does not occur until well above the design serviceability loads; and that, as expected, the attainment of the design ultimate loads relies on there being sufficient post-buckling rotation to shed at least 20 per cent of the peak hogging bending moment into the adjacent midspan regions. The results also show that the load factor at failure, λ_f, is in general higher for the stockier cross-sections of the SB series (range 1.13 to 1.24, with mean value 1.16), than for the TB series (range 1.05 to 1.20 with mean value 1.10). No beam could be found with $\lambda_f < 1.05$.

5.2 Residual Stresses

Rotter has reported [6] that residual stresses in rolled sections tend to increase curvatures at intermediate load levels by up to 25 per cent; but comparison of results of analyses with and without residual stresses showed that they cause only small decreases in λ_f. The largest reductions were 3.5 per cent for the SB series and 9 per cent for the TB series.

5.3 Span ratio

There was no obvious relationship between λ_f and the ratio between the two spans. This is probably because the design loads w_1 and w_2 are influenced in a complex way by span ratio, as well as having the expected reduction with increasing span. The total length L_1+L_2 has negligible effect; similar values of λ_f were obtained for two beams in the TB series with total lengths of 16m and 35m. Span ratios below 0.6 have not been studied; but for these, beams of uniform section would rarely be used.

5.4 Unpropped construction

For a given beam and total load, unpropped construction gives higher stresses in steel and earlier local buckling as discussed by Yam [7]. The method of draft Eurocode 4 takes account of these higher stresses. They are allowed for here (Appendix B) in the calculation of w_1 and w_2, giving values (Table 4) which are lower than for propped construction. The computed buckling and failure loads are also lower (by 4 to 12 per cent and 2.6 to 10 per cent, respectively), but the values λ_b and λ_f, which are the ratios of these loads to w_1 and w_2, are slightly higher than for propped construction. The method of EC4 is thus slightly more conservative for unpropped than for propped construction.

5.5 Sensitivity of λ_f to the slopes of the falling branch

The values of θ'_b computed here are the inelastic rotations at the internal supports when the maximum moment reaches M'_y and the load factor is λ_b. Further increase of load level depends on the steepness of the falling branch of the $M'-\theta'$ curve. A separate study was made of the sensitivity of the results for λ_f to the shape of this falling branch (Figure 2). The effect of increasing the inelastic rotation at $0.6\ M'_y$ from $10\theta'_b$ to $16\theta'_b$ was to increase λ_f by less than 5 per cent in all cases. The assumed $M'-\theta'$ curves are considered to be sufficiently conservative, in view of this insensitivity.

5.6 Combined bending and shear

For ultimate strength in combined bending and shear in Class 3 sections, draft Eurocode 4 refers to Eurocode 3. This is certainly too conservative for composite sections in hogging bending [2]. The method of BS 5400:Part 3 [8], based on tension-field theory, is more appropriate. For the beams in this study it shows that no reduction in M'_y need be made until V/V_{pl} exceeds 0.68. The highest ratio found in these beams, as designed for flexure to Eurocode 4, was 0.57.

5.7 Comments on the design method of draft Eurocode 4

In design practice, instead of calculating the load-carrying capacity of a beam with known cross-sections, the required cross-sections are chosen such that the extreme-fibre stresses in the steel do not exceed yield under various possible loading cases. Usually, the actual design loads are lower than the loads w_1 and w_2 used here, because in practice the ratio w_1/w_2 is known initially. Furthermore, it is possible for a class 3 cross-section to have a moment of resistance above M'_y.

These are further reasons why the present study is a more severe test of the design method than would be likely to occur in practice.

6. CONCLUSIONS

Forty-three two-span continuous composite beams with semi-compact sections at the internal support, and ten different cross sections, have been designed for flexural failure at the ultimate limit state by the less conservative of the two methods given in draft Eurocode 4. These designs correspond to a load factor $\lambda_f = 1$. Spans ranged from 6m to 20m and span ratios from 0.6 to 1.0.

The ultimate strengths of these beams were determined by an inelastic method that takes account of the loss of strength in hogging bending caused by local buckling, determined from laboratory tests on five double cantilevers. The effects of residual stresses and unpropped construction were studied, and were found to have little influence on values of λ_f for the beams, which ranged from 1.05 to 1.33.

For both propped and unpropped construction, local buckling was found not to occur until well above service load levels. The 47 values of λ_b were all between 0.77 and 0.84, except for one value of 0.98, for one of the beams with the highest ratio of slab reinforcement ($A_r/b_c h_c = 0.02$).

This new method from draft Eurocode 4 was found to be both safe and economical for design for the ultimate limit state, and to reflect the real behaviour of two-span beams. For beams of more than two spans, it is believed to be slightly more conservative. The method provides an alternative to the over-conservative design of Class 3 beams that results from the exclusive use (in current practice) of elastic theory.

7. APPENDICES

A. Prediction of M'-θ' curves for SB series of tests on cantilevers

The stress-strain curves used for concrete and reinforcement (Figure A1) were as given in Reference 8. The curve for structural steel (Figure A2(a)) is similar to that used in Reference 9, but modified to be more appropriate for the yield strengths given in Tables 1 and 2.

The cantilevers were similar in section to that shown in Figure 2, with a welded plate simulating the reinforcement and the cracked concrete slab. The residual stresses in the steel section were assumed to be as shown in Figure A2(b), with a compressive stress of $\sigma_y/2$ at the tips of the flanges. The effect of the welds was neglected, being remote from the region that buckled.

The values M'_y and θ'_e (Figure 2) were found by conventional linear-elastic theory.

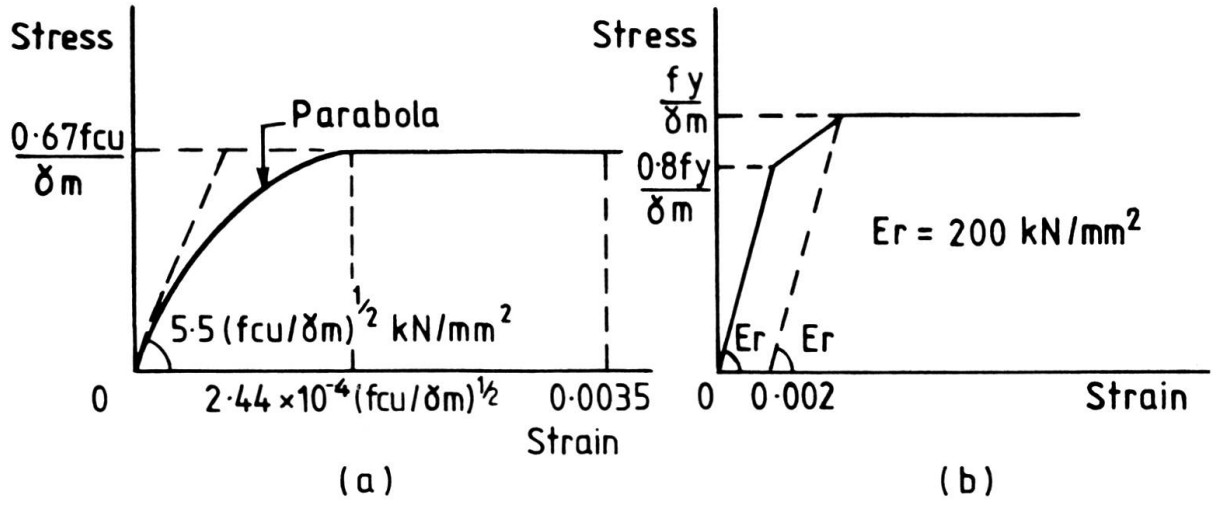

Fig. A1 Stress–strain curves; (a) concrete; (b) reinforcement

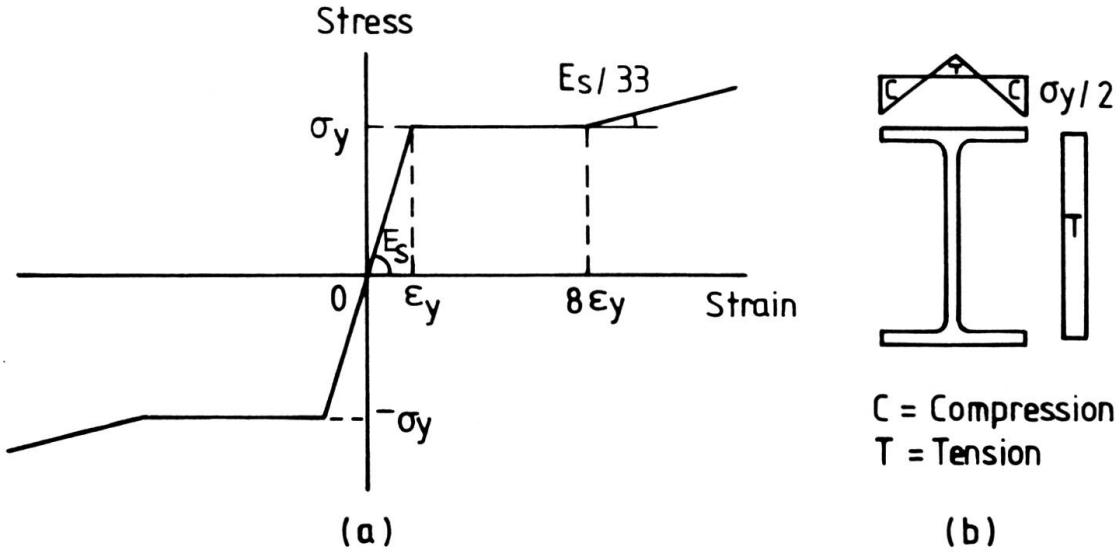

Fig. A2 Structural steel material properties (a) stress–strain curve; (b) residual stress pattern

Thus,

$$\theta'_e = M'_y L/2E_s I_c$$

where L is the length of the cantilever, I_c is the second moment of area of the "cracked reinforced" composite section, and E_s = 205 kN/mm².

The curve NP (Figure 2) was computed from first principles, assuming plane sections remain plane. The rotation θ'_{bc} is thus due to yielding caused by residual stresses and, for true composite sections, to the reduced stiffness of reinforcement at stresses exceeding $0.8\ f_y/\gamma_m$, (Figure A.1(b)). No account was taken of tension stiffening.

Specimen No.	θ'_i/θ'_{bc} at:		Slendernesses:	
	$0.8\ M'_y$	$0.6\ M'_y$	b_o/t	$\alpha d/w$
SB4	4.8	12.2	14.1	34.5
SB5	3.8	11.5	14.9	39.8
SB6	3.7	11.7	16.7	42.7
SB10	4.0	11.1	14.1	33.0
SB11	5.7	14.3	14.9	35.1

Table A1 Observed rotation ratios

The resulting $M'-\theta'$ curves (NPQR in Figure 2) were checked by comparing the predicted inelastic rotation ratios θ'_i/θ'_{bc} (4.0 at $0.8M'_y$ and 10.0 at $0.6M'_y$) with the observed ratios (Table A1). The value 10 is always conservative (i.e., it underestimates the inelastic rotation) and the value 4 is a good approximation. The discrepancies indicate that there is no simple relationship between θ'_i/θ'_{bc} and the slendernesses of the bottom flange or the web.

B. Calculation of design ultimate loads w_1 and w_2 in accordance with method (a) of clause 4.4.3.2 of draft Eurocode 4

The method specifies linear elastic analysis only, except that up to 20 per cent of the peak hogging moments may be redistributed to adjacent midspan regions. For a two-span beam, flexural stiffnesses are as in Figure 3, where I_c and I_u relate to the cracked reinforced and uncracked composite sections respectively. The limiting bending resistances are M'_y (hogging) and M_y (sagging), and $L_2 \geq L_1$. For short-term loading, the modular ratio is taken as 7.5 in the calculation of M_y. Initially, propped construction is assumed.

Maximum loading on the right span is considered first. After redistribution, it is assumed to cause moments M'_y at C and M_y at D (Figure B1 curve 1). Equilibrium then gives the value of load w_2. Before redistribution, the bending moment at C is $1.25\ M'_y$ and the elastic curvatures along CDE are known (Figure B1 curve 2). The maximum loading on span AC, w_1, is then found from the condition that the curvatures along ABC are such that the deflection of point C relative to line AE is zero. It is then checked that $M_B \leq M_y$. Any higher loading on AC would increase M' at C. It is then checked that with the minimum possible loading on AC, and without redistribution, the moment at D is not excessive. Moment-shear interaction is discussed in Section 5.6.

For unpropped construction, the design dead load ($1.35g$, with $g=g_1=g_2$) is first applied to the steel member alone, acting elastically. The relevant extreme fibre stresses are then deducted from the yield stress σ_y, to obtain the allowable stresses in both hogging and sagging bending for the composite section. The imposed load $1.5q_2$ is then found, as above, for span L_2 using composite section properties and equilibrium. The load $1.5q_1$ for span L_1 is found by elastic analysis of the two-span composite member, as above for w_1.

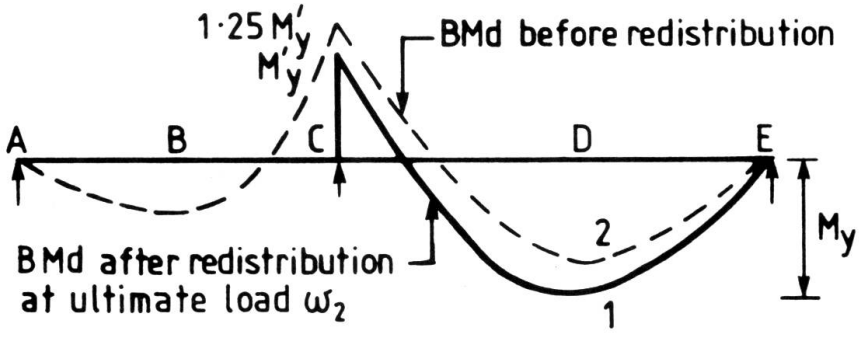

Fig. B1 Redistribution of support moment

C. Calculation of λ_b, θ'_b and λ_f for two-span beam

The geometry, materials, and loads w_1 and w_2 are known. The stress-strain curves and residual stresses are as in Appendix A, except that γ_m is taken as 1.5 for concrete in compression and 1.15 for reinforcement. Slip is neglected.

The method for λ_b is iterative, as follows.

(1) Guess λ (lower than the expected λ_b). The loads λw_1 and λw_2 are then known.

(2) Guess the moment at support C, M'_c, so all moments are known.

(3) Compute all curvatures, and adjust M'_c until a compatible solution is found.

(4) Compare M'_c with M'_y, modify λ, and iterate until a solution is found with $M'_c = M'_y$.

This solution gives λ_b, and a distribution of moments and curvatures along the beam that includes the effects of cracking of concrete and some local yielding.

The irreversible components of these curvatures occur mainly near the internal support, where stresses in steel and reinforcement are much higher than elsewhere. They will now be represented by two concentrated rotations θ'_b at points $h_a/2$ on each side of support C, determined for load level λ_b as follows.

The curvatures in sagging regions are unaltered, but in hogging regions a new set is found, neglecting residual stresses and assuming linear-elastic behaviour with stiffness $\frac{1}{2}E_s(I_c+I_u)$, where I_u is calculated taking E for concrete from the initial slope of the stress-strain curve in Figure A1, with $\gamma_m = 1.5$. The angle $2\theta'_b$ is given by the concentrated rotation at or near point C that makes these new curvatures compatible.

The load factor at failure, λ_f, is found by iterative calculations similar to those for λ_b, but allowing for local buckling in span CE and elastic unloading in the hogging region of span AC. As λ increases above λ_b, the initial guessed value for M'_c is reduced below M'_y, and two concentrated rotations are included in the compatibility checks. When the moment at C is M'_c, Figure C1, these rotations are TU in the non-buckling span and TV in the buckling span.

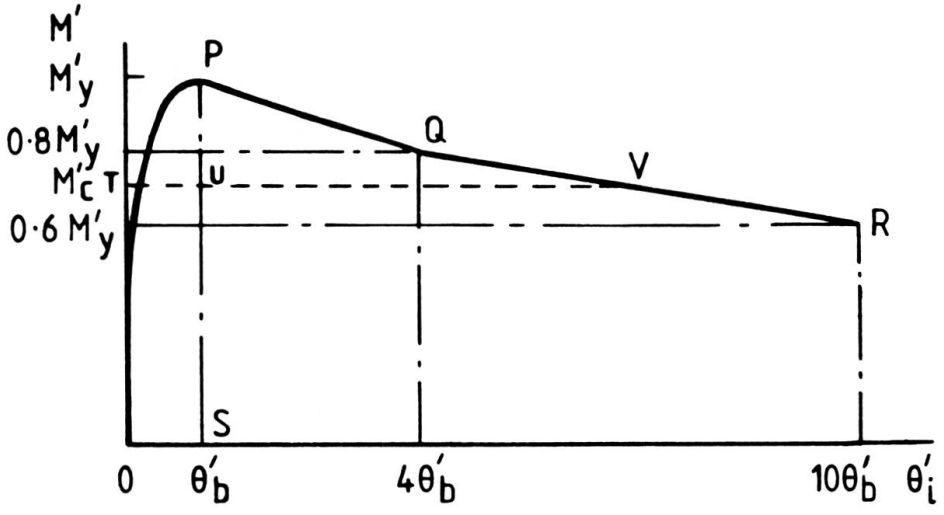

Fig. C1 Irreversible rotations

The failure load ($\lambda = \lambda_f$) is assumed to be reached when either

(i) M'_c drops below $0.6M'_y$,

(ii) the maximum compressive strain in concrete reaches 0.0035,

(iii) the maximum stress in structural steel reaches $1.3\ \sigma_y$, or

(iv) the iteration for a new load increment fails to converge.

D. Extract from clause 4.4.3.2 of draft Eurocode 4, related to design of beams with sections in Class 3

Method (a): Flexural stiffnesses are taken as the cracked values, as defined in 4.4.4.2, over 15% of the span on each side of an internal support, and as the uncracked values elsewhere. The resulting bending moment at each internal support (except those adjacent to cantilevers) may optionally be reduced by up to 20%, and corresponding increases made to the sagging bending moments elsewhere.

NOTATION

A_r total area of longitudinal reinforcement

b_c, h_c breadth and depth of concrete slab (Figure 4)

b_o, d, h_a, t, w dimensions of steel section (Figure 4)

f_{cu} characteristic cube strength of concrete

f_y nominal yield stress of reinforcement

I_c, I_u cracked and uncracked second moments of area of composite cross-section

M' hogging bending moment at an internal support

M'_m peak hogging moment in cantilever tests

M_p, M_y plastic and first yield sagging moments of resistance

M_y' first yield hogging moment of resistance

V, V_{pl} maximum shear force and shear capacity

w_1, w_2 design loads (Figure 3)

L_1, L_2 span lengths of a two-span beam (Figure 3)

αd depth of web in compression (elastic theory)

γ_m partial safety factor for a material

θ' total rotation at the end of a cantilever or at a point of contraflexure

θ'_b irreversible rotation of a quasi-cantilever in a continuous beam when $M' = M'_y$

θ'_{bc} irreversible rotation of a cantilever when $M' = M'_y$ (Figure 2)

θ'_e elastic rotation (Figure 2)

λ_b, λ_f buckling and failure load factors

σ_y nominal yield stress of structural steel

REFERENCES

1. EUROCODE No. 4, Common unified rules for composite steel and concrete structures, draft, Commission of the European Communities, 1985.

2. ALLISON R.W., et al, Tension-field action in composite plate girders, Proc.Instn.Civ.Engrs., Part 2, 73, 255-276, June 1982.

3. HOLTZ N.M. and KULAK G.L., Web slenderness limits of non-compact beams, Structural Engineering Report No. 51, Dept. of Civ. Engrg., University of Alberta, Aug. 1975.

4. NASH D.S. and KULAK G.L., Web slenderness limits for non-compact beam-columns, Structural Engineering Report No. 53, Dept. of Civ. Engrg., University of Alberta. Mar. 1976.

5. CLIMENHAGA J.J. and JOHNSON R.P., Local buckling in continuous composite beams, The Structural Engineer, Vol. 50, No. 9, 367-374, Sept. 1972.

6. ROTTER J.M. and ANSOURIAN P., Cross-section behaviour and ductility in composite beams, Proc.Instn.Civ.Engrs., Part 2, 67, 453-474, June 1979.

7. YAM L.C.P., Design of composite steel-concrete structures, Surrey University Press, London, 1981.

8. BS5400 : Steel, concrete and composite bridges - Part 3 : Design of steel bridges, 1982; Part 4 : Design of concrete bridges; 1984; British Standards Institution, London.

9. ECCS - Technical Committee 8 - Structural Stability, Ultimate limit state calculation of sway frames with rigid joints, Report No. 33, European Convention for Constructional Steelwork, Brussels, 1984.